



# Label-free real-time acoustic sensing of microvesicle release from prostate cancer (PC3) cells using a Quartz Crystal Microbalance



Dan Stratton<sup>a</sup>, Sigrun Lange<sup>b</sup>, Sharad Kholia<sup>a</sup>, Samireh Jorfi<sup>a</sup>, Samuel Antwi-Baffour<sup>a,1</sup>, Jameel Inal<sup>a,\*</sup>

<sup>a</sup> Cellular and Molecular Immunology Research Centre, School of Human Sciences, London Metropolitan University, London, UK

<sup>b</sup> University College London School of Pharmacy, 29-39 Brunswick Square, London WC1N 1AX, UK

## ARTICLE INFO

### Article history:

Received 12 September 2014

Available online 6 October 2014

### Keywords:

Microvesicles

Stimulated release

Real-time analysis

Quartz Crystal Microbalance

Prostate cancer cells (PC3)

## ABSTRACT

Using a Quartz Crystal Microbalance with dissipation monitoring, QCM-D (label-free system) measuring changes in resonant frequency ( $\Delta f$ ) that equate to mass deposited on a sensor, we showed the attachment, over a 60 min period, of a monolayer of PC3 cells to the gold electrodes of the quartz crystal sensor, which had been rendered hydrophilic. That MVs were released upon BzATP stimulation of cells was confirmed by NTA analysis (average 250 nm diameter), flow cytometry, showing high phosphatidylserine exposition and by fluorescent (Annexin V Alexa Fluor<sup>®</sup> 488-positive) and electron microscopy. Over a period of 1000s (16.7 min) during which early apoptosis increased from 4% plateauing at 10% and late apoptosis rose to 2%, the  $\Delta f$  increased 20 Hz, thereupon remaining constant for the last 1000s of the experiment. Using the Sauerbrey equation, the loss in mass, which corresponded to the release of  $2.36 \times 10^6$  MVs, was calculated to be 23 ng. We therefore estimated the mass of an MV to be 0.24 pg. With the deposition on the QCM-D of  $3.5 \times 10^7$  MVs over 200s, the decrease in  $\Delta f$  (Hz) gave an estimate of 0.235 pg per MV.

© 2014 Elsevier Inc. All rights reserved.

## 1. Introduction

Cells typically produce a variety of vesicles, some of which, including lysosomes, endosomes, multivesicular bodies and various transport and secretory vehicles remain within the cell. Of those that are released, exosomes are distinguished from microvesicles (MVs) by their smaller size, 50–100 nm, lower expression of phosphatidylserine (PtSer) and by expression of the surface markers Alix, CD63 and TSG101 [1]. The established characteristics for MVs include size,  $\sim 0.1$ – $1 \mu\text{m}$  in diameter, and for all MVs, regardless of cellular origin, the expression of negatively charged phospholipids such as phosphatidylserine and phosphatidylcholine (PC) translocated on to the outer leaflet of the plasma membrane [1]. This is seen during early apoptosis [2] a feature with which MV release seems to be associated [3]. MVs may be enriched for phospho- and bioactive-lipids, depending on stimulus or cell type [4,5] and contain RNAs and cytoplasmic enzymes as well as cytoskeletal proteins [1,6]. The cytokines and receptors MVs carry are

characteristic of their cellular origin [1], and they are important vectors of intercellular communication, with roles in cancer progression and resistance [7], infectious disease [8–10] and autoimmune disease [11].

The Quartz Crystal Microbalance (ACM) is an acoustic biosensor which monitors mass changes on a quartz crystal sensor surface. This extremely sensitive piezoelectric device is able to detect mass coupled to the surface of the sensor (either adhered or adsorbed). It enables a label-free monitoring in real-time of cell attachment kinetics and also of spreading on different sensor coatings. Of more interest to the current study to monitor MV release from stimulated cells, the QCM with dissipation monitoring (QCM-D) has been used to monitor cell responses to cytomorphic agents causing cytoskeletal changes to primary endothelial cells and fibroblasts [12,13]. For uniform and thin adsorptions onto the sensor, the variation in resonance frequency of the sensor ( $\Delta f$ ) is proportional to the adsorbed mass. In terms of cells, they have to be in direct contact with the sensor surface and not just settled onto a cell layer in direct contact with the sensor surface [14]. The QCM-D can also directly monitor energy dissipation ( $D$ ) as a measure of the viscoelastic properties of the deposited cells; the change in dissipation factor ( $\Delta D$ ) is essentially defined as the ratio of the dissipated energy to the stored or elastic energy per cycle of vibration due to a pulse of current. Of specific interest to the use of the QCM-D to monitor microvesiculation, the device has already been used

\* Corresponding author at: Cellular and Molecular Immunology Research Centre, School of Health Sciences, London Metropolitan University, 166-220 Holloway Road, London N7 8DB, UK.

E-mail address: [j.inal@londonmet.ac.uk](mailto:j.inal@londonmet.ac.uk) (J. Inal).

<sup>1</sup> Current address: School of Allied Health Sciences, College of Health Sciences, University of Ghana, Accra, Ghana.

to measure the dynamics of exocytosis from PC 12 and NG 108-15 cells, stimulated by increased potassium concentration and spontaneous endocytosis [15]. In this study we are able to show a real-time loss in mass and decrease in viscoelasticity of cells stimulated to release MVs and to use the QCM-D to make estimations of the mass of a MV.

## 2. Materials and methods

### 2.1. Cell culturing

The PC3 cells were grown in Dulbecco's modified Eagle medium (DMEM) with extracellular vesicle-free 10% fetal bovine serum (FBS) at 37 °C (5% CO<sub>2</sub> and humidified conditions). The cells were detached from the flasks using trypsin and then resuspended in serum-free DMEM to eliminate serum-mediated interactions with the electrode, washed, counted and injected into the QCM-D chamber.

### 2.2. Isolation of constitutively released MVs

PC3 cells (used between passage 3 and 8) were cultured and MVs isolated as described before [16,17]. Essentially, for MV isolation, stimulated cells in culture medium comprising DMEM with 5% extracellular vesicle- (EV-) free FBS (rendered MV- and exosome-free (EV-free) by centrifugation at 4000g, filtration using a 0.22 µm filter and centrifugation at 160,000g for 90 min) were separated by centrifugation at 160g for 5 min and then again twice more at 4000g for 60 min; the supernatant was immediately centrifuged at 25,000g for 90 min. The resulting supernatant was then discarded, and the pellet suspended in 250 µl sterile, EV-free PBS

before a final centrifugation at 25,000g for 15 min. The resulting pellet, suspended in 100 µl sterile EV-free Dulbecco's PBS (Mg<sup>2+</sup> and Ca<sup>2+</sup>-free) was labelled with Annexin V (see labelling for PtSer below) and quantified on the Guava EasyCyte 8HT flow cytometer (and ExpressPlus software) which uses a stepper motor pump, therefore taking up an exact volume. To avoid the counting of any large debris and MVs together, fluorescent or autofluorescent MVs were always gated. When the FSC versus SSC plot was observed with this gate applied, so called 'backgating,' any debris was thus excluded.

### 2.3. Stimulation of cells with BzATP

To stimulate MV release with BzATP, cells ( $1 \times 10^5$  cells/ml) in pre-warmed DMEM and 2 mM CaCl<sub>2</sub> were stimulated with 200 µM BzATP (37 °C) in the presence of 2 mM CaCl<sub>2</sub>. Released MVs were recovered by differential centrifugation and quantified as described above.

### 2.4. Labelling for PtSer and electron microscopy

For detection of phosphatidylserine, MVs were labelled with fluorescein-conjugated Annexin V as described before [9,11,16]. Samples for electron microscopy were also prepared for negative staining as described before [9] and viewed using a JEOL JEM-1200 EX II transmission electron microscope.

### 2.5. Fluorescent microscopy analysis

Annexin V Alexa Fluor<sup>®</sup> 488 was diluted in the manufacturer's binding buffer (eBiosciences) and used at 1 µg/10<sup>6</sup> cells, according

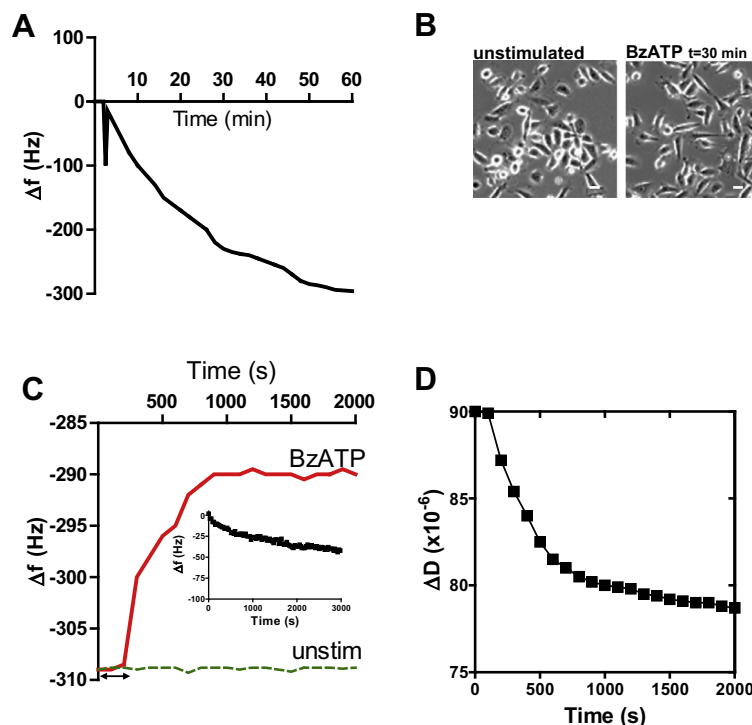


**Fig. 1.** Time course of mass loss and decrease in dissipated energy  $\Delta D$  (viscoelasticity) from PC3 cells stimulated with BzATP, as measured using the QCM-D. (A) Using sub-harmonic F<sub>1:1</sub>, the mass of the PC3 cells measured increases as the cells ( $1 \times 10^5$ ) settle onto the sensor, there being a sharp increase over 0–60 min. At the 60 min time point (B) the cells were stimulated to microvesiculate with BzATP (200 µM) and observed by light microscopy to show continued attachment; bar, 10 µm. Stimulation with BzATP, or sublytic complement (5% NHS) which gave the same graph, is shown in (C), and indicates a sharp loss in mass (decrease in frequency) after a 100s lag phase, indicated by a double-headed arrow, up to 1000s post stimulus (red line). This loss in mass remains constant thereafter. The dashed line represents  $1 \times 10^5$  cells similarly deposited on the crystal but this time not stimulated (or stimulated with heat inactivated NHS, where appropriate). The baseline without cells is shown inset. (D) Using sub-harmonic D<sub>1:1</sub> on the QCM-D, the changes in the dissipation factor,  $\Delta D$ , indicating the changes in the levels of dissipated energy of the PC3 cells after stimulation with BzATP, were monitored. (For interpretation of the references to colour in this figure legend, the reader is referred to the web version of this article.)

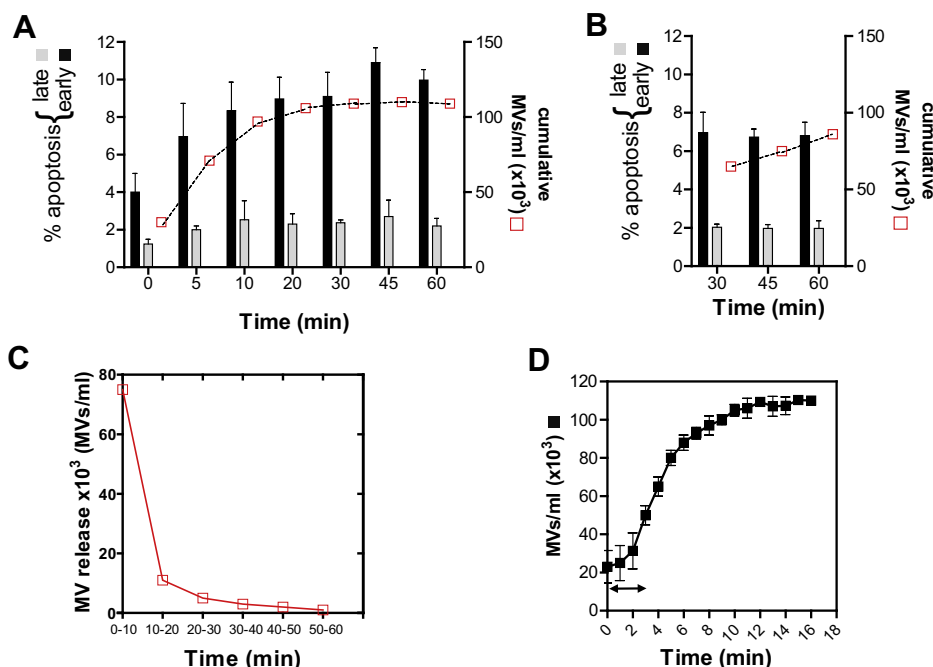


**Fig. 2.** Increases in levels of early apoptosis and of MV release from PC3 cells taper off 20 min after stimulation.  $1 \times 10^5$  cells were treated with 200  $\mu$ M BzATP (or 5% NHS) and levels of early (AnV<sup>+</sup>) and late (AnV<sup>+</sup> and 7-AAD<sup>+</sup>) apoptosis as well as of cumulative MV levels released, were monitored over 1 h (A) using the Guava EasyCyte. After a 30 min rest period, (B) shows that early apoptosis levels were restored back to resting levels as were levels of MVs released. (C) MV release during every 10 min period over 1 h after BzATP stimulus also shows that after 20 min new MV release has fallen to a minimal basal level. More detailed analysis of MV release over the first 10 min post stimulus (D).

to the manufacturer's instructions. Cells were labelled with AnV Alexa Fluor<sup>®</sup> 488, at room temperature for 15 min with gentle agitation and then washed three times in serum-free RPMI.

## 2.6. Assessment of apoptosis by flow cytometry

To assess the level of apoptosis of cells releasing MVs, cells were stained with annexin V (AnV) and 7-aminoactinomycin D (7-AAD) (Guava Nexin Reagent). Cells positive for AnV only (early apoptotic) or AnV and 7-AAD-positive cells (late apoptotic) were quantified over 60 min using the Guava EasyCyte flow cytometer.

## 2.7. Nanoparticle tracking analysis (NTA) of MVs released from PC3 cells

MVs released after treating PC3 cells with BzATP were collected as described above. NTA was performed using the NanoSight LM20 according to the manufacturer's instructions (NanoSight, U.K.) the vesicles being quantified for size and number.

## 2.8. Quartz Crystal Microbalance (QCM) analysis

To set up the QCM biosensor (Q-Sense E1) the AT cut quartz crystal was made to oscillate at its resonant frequency of 8.85 MHz by applying an AC voltage to a 5 mm diameter gold electrode. The gold surface, a 100 nm polished gold layer coating the quartz crystal, was made hydrophilic as previously described [15]. The QCM disks were then coated on the upper surface with oxidised polystyrene (0.5% w/v in toluene), the QCM being placed in a 37 °C incubator with 5% CO<sub>2</sub>. After stabilizing  $\Delta f$  with pure water and then serum-free DMEM and 2 mM Ca<sup>2+</sup>, PC3 cells were injected onto the electrode at a density of  $2.5 \times 10^4$  cells/ml with a flow rate of 0.1  $\mu$ l/min. Serum-free DMEM was flowed over the cells until a steady baseline was established after 60 min, where-

upon non-adherent cells were removed. Adherent cells were monitored by microscopy at this stage and again after stimulation to microvesiculate, as described below.

The sample halted on the sensor was allowed to microvesiculate by adding 200  $\mu$ M BzATP (or 5% EV-free NHS) while the microbalance recorded changes in sample density and fluid rigidity. QCM analysis of MV density was performed by stimulating the MV sample with 5 MHz (or up to 70 MHz) while monitoring the 3rd (1.486 MHz) sub-harmonic and (which typifies resonance of the sensor) measuring the decrease in amplitude and resonance frequency ( $f$ ). The average density of the MV sample is proportional to the frequency and the loss of amplitude. Any shift in  $\Delta f$  in the QCM relates to changes in mass absorbed onto the crystal. Using the Sauerbrey equation,  $m = -C \left( \frac{\Delta f}{\nu} \right)$ , where the crystal constant,  $C$ , in this case ( $17.7 \text{ ng cm}^{-2} \text{ Hz}^{-1}$ ) is a constant particular to a 5 MHz quartz crystal and  $\nu = 3$  (the third overtone) it is possible to monitor deposition of cells on the crystal as well as release of MVs in a label-free environment.

For *in situ* microscopic monitoring of cells on the crystal sensor, the Q-Sense E1 chamber containing a window module, QWM 401, mounted on an Olympus IX81 microscope, was used according manufacturer's instructions. This allowed for assessment of cell number and morphology.

## 2.9. Statistical analysis

All experiments were carried out in triplicate and repeated two or three times. The data are represented as mean  $\pm$  standard error of the mean. Statistical analysis (unpaired  $t$  test) was performed using version 5.0 of the GraphPad Prism software, (GraphPad Software, San Diego, CA). The following significance levels were used: \* $p < 0.05$ , \*\* $p < 0.01$  and \*\*\* $p < 0.001$ .

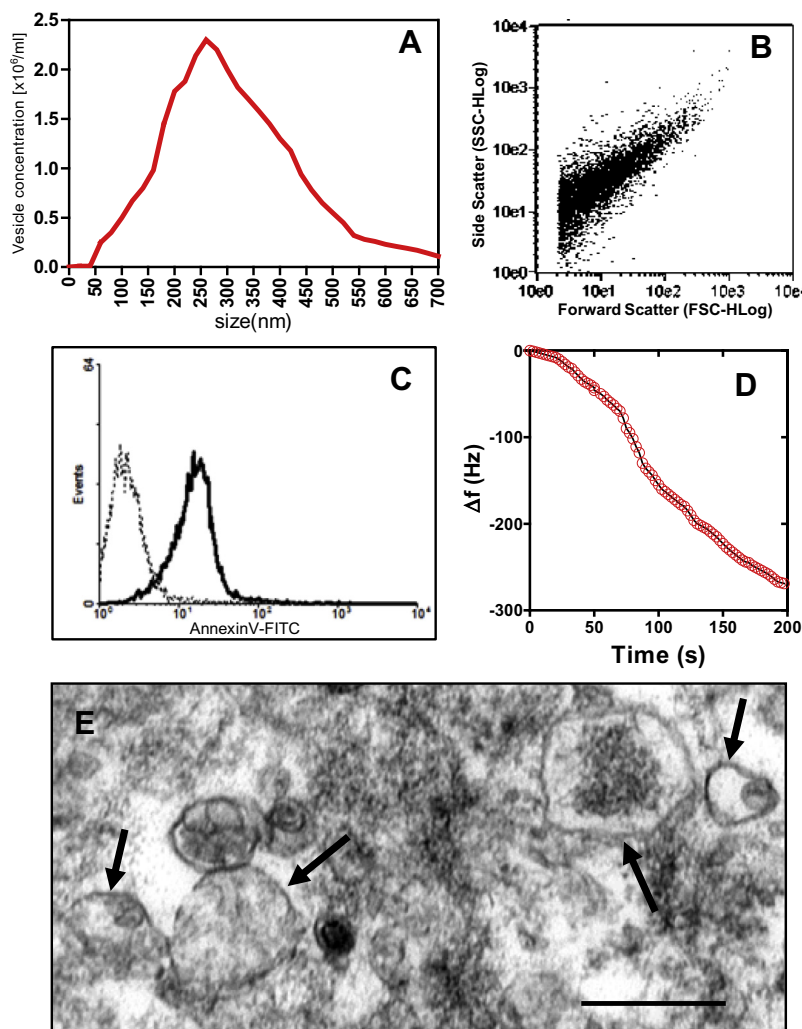


**Fig. 3.** Microvesicles are released from PC3 cells upon stimulation with BzATP. MVs released from cells after treatment with BzATP were collected by centrifugation (160g for 5 min; 4000g for 90 min; 25,000g for 60 min) and then sizes measured (mean values,  $n = 3$ ) using a NanoSight LM20 (nanoparticle tracking analysis, NTA) (A). Vesicles above 100 nm are likely to be mainly MVs. (B) A forward scatter/side scatter dot plot is shown for the MVs isolated after BzATP stimulation showing a typical tapered distribution characteristically showing the heterogenous size range expected for MVs and with a high percentage staining with annexin V-FITC, indicating high exposition of PS, (C). In (D) the QCM was used at a crystal oscillation of 70 MHz to analyse MV mass, suspended in PBS. MVs were analysed for their ability to quench the oscillating momentum on a QCM using F3. Using the Sauerbrey equation and based on the value of  $\Delta f$  obtained for the deposition of  $\sim 10^7$  MVs on the quartz sensor, a value for the average mass of MVs released from BzATP-stimulated PC3 cells was obtained as 0.235 pg. (E) MVs released from BzATP-stimulated PC3 cells were isolated by centrifugation from cell-free supernatants at 25,000g for 60 min. Negative staining was carried out and samples examined on a JEOL JEM-1200 EXII electron microscope; bar, 300 nm.

### 3. Results

#### 3.1. Stimulated PC3 cells undergo maximal MV release and loss of mass, as measured on a QCM-D, within 1000s

During the adsorption phase, over 1 h, (Fig. 1A) the frequency measurement of the QCM decreased due to firm cell attachment to the sensor surface. Microscopic observations of the cells, through the QCM-D window module (Fig. 1B), confirmed no multilayers and no major cell desorption during this period. Having established a confluent cell monolayer we then set about using this as an acoustic biosensing device to monitor loss in mass during microvesiculation.

Essentially we aimed to use the QCM-D to record MV release from cells, in the absence of any labelling or fluorescent probe, by measuring any mass change of the cells. Cells ( $1 \times 10^5$ ), were allowed to deposit onto the gold electrodes of the QCM, at 37 °C, the frequency decrease over the first 1000s indicating cell

attachment (Fig. 1A). The cells (indicated by the red line in Fig. 1C) were then stimulated with 200  $\mu$ M BzATP or not stimulated (green, dashed line). We sometimes used LPS or 5% EV-free NHS in RPMI and  $\text{Ca}^{2+}$  (2 mM) with heat inactivated NHS as control, despite reservation about using deposited membrane attack complex (C5b-9) as used before [16] in experiments to measure mass, and generated very similar results. During the ensuing 1000s, the resonate frequency increased by 19 Hz indicating a loss in mass, which we believe to be consistent with the high rate of MV release indicated in Fig. 2. Data showing QCM-D analysis of MV release from PC3 cells at a second sub-harmonic with emphasis on the periphery of the sensor, which was similar to that in Fig. 1C is not shown. The highly reproducible base line analysis of the PC3 cells is shown inset in Fig. 1C indicating that the cells do not spontaneously lose mass and that the various stimuli used earlier had been required to stimulate MV release. Fig. 1B also shows that the loss in mass observed following microvesiculation, using the QCM-D, is unlikely to be due to cell



detachment or desorption, as cell attachment is largely retained after BzATP stimulation.

### 3.2. The mass of an MV is 0.25 pg as determined using the QCM-D

Given the crystal constant,  $C$ , to be  $17.7 \text{ ng cm}^{-2} \text{ Hz}^{-1}$ ,  $\Delta f$  as 19 Hz (Fig. 1C) and  $\nu$  as 3 (the third overtone), and knowing the crystal area to be  $0.2 \text{ cm}^2$ , using the Sauerbrey equation (Section 2.8) we calculated the overall mass loss from cells to be 23 ng. As this corresponds to  $2.36 \pm 0.09 \times 10^6$  MVs released (average release from  $1 \times 10^5$  cells,  $n = 6$ ), we estimate an MV to have a mass of 0.24 pg.

### 3.3. Loss of dissipation factor levels off 1000s after stimulation of PC3 cells with BzATP

The QCM-D is also able to monitor changes in the dissipation factor,  $\Delta D$ , of deposited cells. Fig. 1D shows the changes in the degree of dissipated energy of the PC3 cells after stimulation with BzATP. Whilst  $\Delta f$  increased with time (Fig. 1C),  $\Delta D$  steadily decreased indicating a decrease in viscoelastic properties. According to earlier findings using A431 cells exposed to EGF [18] this reduction in  $\Delta D$  was likely to be due to remodelling of the actin cytoskeleton [19] which was induced by EGF treatment [18]. Cytoskeletal rearrangements also accounted for decreases in  $\Delta D$  in NIH3T3 fibroblasts [20]. The possibility that the observed decrease in  $\Delta D$  upon BzATP stimulation of P2X7 receptors in PC3 cells could also be due to actin reorganisation certainly exists in view of actin reorganisation and membrane blebbing having been shown to be mediated through p38- and Rho-dependent pathways in RAW 264.7 macrophages [21].

Although it might be that morphological changes in the cells might be more easily detectable than by microscopy, the QCM-D being more sensitive than microscopy, we cannot discount that MVs were detected to be released from the cells, by flow cytometry and TEM.

### 3.4. Within 20 min of stimulus the cessation of MV release coincides with the levelling off of early apoptosis levels (increasing from 4% to 10%)

The 16 min period over which there are increasing levels of MV release as determined on the QCM coincides with the increasing levels of MVs released (Fig. 2), as measured by flow and with increases in early apoptosis. The sharp increase in MV release after an initial lag phase of 1–2 min (Fig. 2D), levelled off 20 min after stimulus (Fig. 2A and C). We found the increase in MV release and consequent loss in mass to coincide with an increase in early apoptosis from 4% plateauing at 10%, levels of cells in late apoptosis increasing from 1% to 2%; levels of cell death below 5% were defined for the purposes of this study as sublytic. That these low levels of apoptosis upon stimulation and MV release are recoverable is shown in Fig. 2 where the stimulated cells used in Fig. 2A were rested for 30 min and placed back in medium without stimulation. These cells showed reduced levels of early apoptosis (10% down to 6%), (Fig. 2B) as well as reduced levels of MV release.

### 3.5. MV release from PC3 cells was monitored by NTA, flow cytometry and fluorescent microscopy (PS exposition), as well as electron microscopy

To confirm that MVs were being released upon BzATP stimulation of PC3 cells (Fig. 3) we analysed the supernatants in parallel experiments of cells stimulated with BzATP (200  $\mu\text{M}$ ) by isolating MVs using differential centrifugation. We then confirmed the presence of MVs by their typical size distribution through NTA (averag-

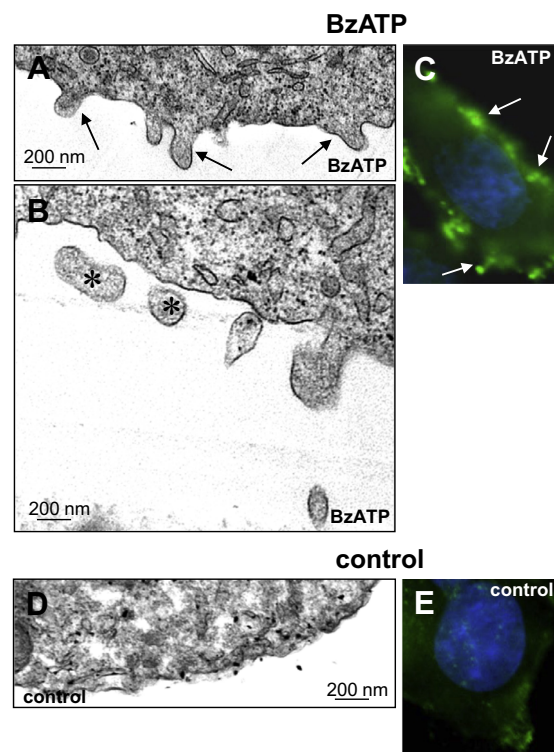


**Fig. 4.** BzATP stimulates budding and MV release from the surface of PC3 cells as seen by transmission electron microscopy and immunofluorescence microscopy. Transmission electron microscopy, original magnification  $\times 100,000$ , shows budding (arrows) (A) and release (asterisk) of MVs from the surface of PC3 cells stimulated with 200  $\mu\text{M}$  BzATP at 37 °C (B). Using fluorescence microscopy, cells stained with annexin V Alexa Fluor<sup>®</sup> 488 and DAPI-VECTASHIELD, original magnification  $\times 10,000$ , also indicate budding and MV release (white arrows) from stimulated cells. Control, untreated cells are shown in (D) and (E).

ing at 250 nm diameter) (Fig. 3A) by flow cytometry (Fig. 3B), indicating a typical scatter plot (side scatter versus forward scatter) for MVs with a heterogeneous, tapering distribution, and which characteristically for MVs had a highly positive signal for annexin V binding (92%) (Fig. 3C), indicating high PS exposition. The MVs ( $3.5 \times 10^7$ ) applied to the QCM-D showed a decrease in  $\Delta f$  of  $-269 \text{ Hz}$  (Fig. 3D) which, using the Sauerbrey equation, equates to an average mass of an MV of 0.235 pg, agreeing remarkably well with the earlier estimate from the loss of mass of stimulated cells. Finally we were able to confirm the presence of MVs by electron microscopy (Fig. 3E). We also showed MV release directly from the PC3 cell surface following BzATP stimulation by electron microscopy (Fig. 4A and B) and by fluorescent microscopy with Alexa Fluor<sup>®</sup> 488 labelled Annexin V (Fig. 4C).

## 4. Discussion

Using the QCM-D we were able to measure a significant change in cellular mass, beginning upon stimulation of PC3 cells with 200  $\mu\text{M}$  BzATP and peaking at 1000s (16 min 40s) post stimulus, a not untypical timescale of MV release. The lag period before MV release, measured using the QCM-D as loss in mass (Fig. 1C) and in terms of MV numbers (Fig. 2D) which was 1–2 min, was reminiscent of lysosomal exocytosis, another  $\text{Ca}^{2+}$ -mediated process involving vesicle movement [22], where there was a 100s delay before calcium-ionophore stimulated and  $\text{Ca}^{2+}$ -mediated lysosomal exocytosis was initiated. The QCM also detected a decrease in media fluidity, attributed to the process of membrane blebbing on THP-1 [23] and MV release. The QCM was able to pro-

vide an accurate measurement of MV mass (0.24 pg) by calculating the loss in mass of the stimulated cells and through direct deposition of isolated MVs on the quartz sensor.

The loss of mass detected by the QCM-D could have been due to cell rounding (likely cell retraction) as was observed for bacterial LPS-treated endothelial cells [12] which would have caused a decrease in mass (increase in  $\Delta f$ , or  $\Delta f_{\text{pos}}$ ) and of dissipation (decrease in  $\Delta D$ ). Increases in frequency responses have also been observed due to stimulation of the cell membrane and resulting vesicle exocytosis [15], detachment of cells from the surface of the sensor [24] and viscosity changes in the cytosol due to changes in the rigidity of the cytoskeleton [25]. These reasons for  $\Delta f_{\text{pos}}$  (losses of mass) are unlikely in this case as microscopy of cells *in situ* in the flow cell of the QCM-D showed no significant change in cell number for BzATP-treated PC3 cells (Fig. 1B).

In summary, this study proposes the use of the QCM-D as a novel tool in the study of cellular vesiculation, providing a label-free, real-time system for detecting MV release as a loss of cellular mass, and for monitoring changes in viscoelasticity of microvesiculating cells as well as of analysing MVs themselves, giving an accurate measure of mass.

## Acknowledgments

We are indebted to members of CMIRC for critically reading the manuscript and to R. Moss for assisting with the electron microscopy. This work was part-funded by the Sir Richard Stapely Educational Trust, the Royal Society and HEFCE QR Funding (RAE2008). SK was a VC scholarship recipient from LMU.

## References

- [1] J.M. Inal, E.A. Ansa-Addo, D. Stratton, S. Kholia, S.S. Antwi-Baffour, S. Jorfi, S. Lange, Microvesicles in health and disease, *Arch. Immunol. Ther. Exp. (Warsz)* 60 (2012) 107–121.
- [2] D.L. Bratton, V.A. Fadok, D.A. Richter, J.M. Kailey, L.A. Guthrie, P.M. Henson, Appearance of phosphatidylserine on apoptotic cells requires calcium-mediated nonspecific flip-flop and is enhanced by loss of the aminophospholipid translocase, *J. Biol. Chem.* 272 (1997) 26159–26165.
- [3] D. Stratton, S. Lange, J.M. Inal, Pulsed extremely low-frequency magnetic fields stimulate microvesicle release from human monocytic leukaemia cells, *Biochem. Biophys. Res. Commun.* 430 (2013) 470–475.
- [4] N. Aoki, S. Jin-no, Y. Nakagawa, N. Asai, E. Arakawa, N. Tamura, T. Tamura, T. Matsuda, Identification and characterization of microvesicles secreted by 3T3-L1 adipocytes: redox- and hormone-dependent induction of milk fat globule-epidermal growth factor 8-associated microvesicles, *Endocrinology* 148 (2007) 3850–3862.
- [5] S. Nolan, R. Dixon, K. Norman, P. Hellewell, V. Ridger, Nitric oxide regulates neutrophil migration through microparticle formation, *Am. J. Pathol.* 172 (2008) 265–273.
- [6] J.M. Inal, U. Kosgodage, S. Azam, D. Stratton, S. Antwi-Baffour, S. Lange, Blood/plasma secretome and microvesicles, *Biochim. Biophys. Acta* 1834 (2013) 2317–2325.
- [7] S. Jorfi, J.M. Inal, The role of microvesicles in cancer progression and drug resistance, *Biochem. Soc. Trans.* 41 (2013) 293–298.
- [8] J.M. Inal, S. Jorfi, Coxsackievirus B transmission and possible new roles for extracellular vesicles, *Biochem. Soc. Trans.* 41 (2013) 299–302.
- [9] I. Cestari, E. Ansa-Addo, P. Deolindo, J.M. Inal, M.I. Ramirez, *Trypanosoma cruzi* immune evasion mediated by host cell-derived microvesicles, *J. Immunol.* 188 (2012) 1942–1952.
- [10] J.M. Inal, E.A. Ansa-Addo, S. Lange, Interplay of host-pathogen microvesicles and their role in infectious disease, *Biochem. Soc. Trans.* 41 (2013) 258–262.
- [11] S. Antwi-Baffour, S. Kholia, Y.K. Aryee, E.A. Ansa-Addo, D. Stratton, S. Lange, J.M. Inal, Human plasma membrane-derived vesicles inhibit the phagocytosis of apoptotic cells – possible role in SLE, *Biochem. Biophys. Res. Commun.* 398 (2010) 278–283.
- [12] J. Fattison, F. Azari, N. Tufenkji, Real-time QCM-D monitoring of cellular responses to different cytomorphic agents, *Biosens. Bioelectron.* 26 (2011) 3207–3212.
- [13] K.A. Marx, T. Zhou, A. Montrone, H. Schulze, S.J. Braunhut, A quartz crystal microbalance cell biosensor: detection of microtubule alterations in living cells at nM nocodazole concentrations, *Biosens. Bioelectron.* 16 (2001) 773–782.
- [14] J. Wegener, A. Janshoff, H.J. Galla, Cell adhesion monitoring using a quartz crystal microbalance: comparative analysis of different mammalian cell lines, *Eur. Biophys. J.* 28 (1999) 26–37.
- [15] A.S. Cans, F. Hook, O. Shupliakov, A.G. Ewing, P.S. Eriksson, L. Brodin, O. Orwar, Measurement of the dynamics of exocytosis and vesicle retrieval at cell populations using a quartz crystal microbalance, *Anal. Chem.* 73 (2001) 5805–5811.
- [16] E.A. Ansa-Addo, S. Lange, D. Stratton, S. Antwi-Baffour, I. Cestari, M.I. Ramirez, M.V. McCrossan, J.M. Inal, Human plasma membrane-derived vesicles halt proliferation and induce differentiation of THP-1 acute monocytic leukemia cells, *J. Immunol.* 185 (2010) 5236–5246.
- [17] R. Grant, E. Ansa-Addo, D. Stratton, S. Antwi-Baffour, S. Jorfi, S. Kholia, L. Krige, S. Lange, J. Inal, A filtration-based protocol to isolate human plasma membrane-derived vesicles and exosomes from blood plasma, *J. Immunol. Methods* 371 (2011) 143–151.
- [18] J.Y. Chen, M. Li, L.S. Penn, J. Xi, Real-time and label-free detection of cellular response to signaling mediated by distinct subclasses of epidermal growth factor receptors, *Anal. Chem.* 83 (2011) 3141–3146.
- [19] T.G. Kuznetsova, M.N. Starodubtseva, N.I. Yegorenkov, S.A. Chizhik, R.I. Zhdanov, Atomic force microscopy probing of cell elasticity, *Micron* 38 (2007) 824–833.
- [20] N. Tymchenko, E. Nileback, M.V. Voinova, J. Gold, B. Kasemo, S. Svedhem, Reversible changes in cell morphology due to cytoskeletal rearrangements measured in real-time by QCM-D, *Biointerphases* 7 (2012) 43.
- [21] Z.A. Pfeiffer, M. Aga, U. Prabhu, J.J. Watters, D.J. Hall, P.J. Bertics, The nucleotide receptor P2X7 mediates actin reorganization and membrane blebbing in RAW 264.7 macrophages via p38 MAP kinase and Rho, *J. Leukoc. Biol.* 75 (2004) 1173–1182.
- [22] J.K. Jaiswal, N.W. Andrews, S.M. Simon, Membrane proximal lysosomes are the major vesicles responsible for calcium-dependent exocytosis in nonsecretory cells, *J. Cell Biol.* 159 (2002) 625–635.
- [23] A.B. Mackenzie, M.T. Young, E. Adinolfi, A. Surprenant, Pseudoapoptosis induced by brief activation of ATP-gated P2X7 receptors, *J. Biol. Chem.* 280 (2005) 33968–33976.
- [24] K.A. Marx, T. Zhou, A. Montrone, D. McIntosh, S.J. Braunhut, Quartz crystal microbalance biosensor study of endothelial cells and their extracellular matrix following cell removal: evidence for transient cellular stress and viscoelastic changes during detachment and the elastic behavior of the pure matrix, *Anal. Biochem.* 343 (2005) 23–34.
- [25] C. Galli Marxer, M. Collaud Coen, T. Greber, U.F. Greber, L. Schlappbach, Cell spreading on quartz crystal microbalance elicits positive frequency shifts indicative of viscosity changes, *Anal. Bioanal. Chem.* 377 (2003) 578–586.